Effect of cryogenic friction conditions on surface quality

El Mehdi Skalante, Hamid Makich, Mohammed Nouari

Available online at www.sciencedirect.com

ScienceDirect

Procedia CIRP 00 (2022) 000–000

www.elsevier.com/locate/procedia

6th CIRP Conference on Surface Integrity

Effect of cryogenic friction conditions on surface quality

El Mehdi Skalante[a], Hamid Makich[a,*], Mohammed Nouari[a]

[a]*Université de Lorraine, CNRS, LEM3, IMT-GIP InSIC, F-88100, Saint Dié des Vosges, France*

* Corresponding author. Tel.: +33 (0)329 421 821; fax: +33 (0)329 421 825. *E-mail address:* hamid.makich@univ.lorraine.fr

Abstract

This paper presents an experimental investigation on the tribological behavior of titanium alloys under cryogenic lubrication. The main goal of the study is to reproduce of thermomechanical loading encountered during a cryogenic machining operation. A tribological characterization was performed on a designed tribology system that allows contact between parts and wear tests under different controlled environments (hot temperature, lubrication, cryogenic, humidity, …). The experimental bench has been equipped with the cryogenic fluid routing in the friction zone. A detailed analysis of the surfaces damage of the samples was then carried out to highlight the effects of the loading conditions on the surface integrity. The friction coefficient and wear volume are deeply analyzed to identify physical phenomena governing dry and cryogenic contacts.

Keywords: cryogenic condition, friction interaction, surface damage;

1. Introduction

Nomenclature

MQL	Minimum quantity of lubrication
TA6V	Titanium alloy Ti-6Al-4V ELI grade 5
WC/Co	Tungsten carbide grade 10 K15
LN_2	Liquid nitrogen
F_z	Normal force applied in pin-on-disk tests
F_x	Tangential force measured during friction
μ	Coefficient of friction

Tribological behavior in machining is the subject of several studies to improve the life of tools subject to wear, optimize the surface integrity of the machined part and minimize the energy required for cutting. [1], [2]. Conventional machining of titanium alloys induces severe tool wear mechanisms that subsequently affect the surface integrity of the machined parts [3]. To counteract these thermomechanical wear phenomena, new lubrication technologies are the focus of research and development of high speed assisted machining. In this context, cryogenic assistance is emerging in machining field [4]. The cooling capability of cryogenic fluids is due to their very low vaporization temperature [5]. Several studies focussed on the effect of cryogenic assistance on the machining performance and the surface integrity of the machined parts.

The study carried out by Hong [6] stipulates the existence of two mechanisms: thermal and hydrodynamic, which are responsible of the decrease in the friction coefficient under cryogenic conditions in comparison with dry friction. The thermal effect induces a gain in hardness of the antagonistic surfaces and attenuates the adhesion between the two bodies in contact. The second hydrodynamic effect of lubrication is the formation of a gas phase film between asperities. However, this hypothesis is often discussed because of two reasons: the first is that the contact pressure tested by Hong [6] does not represent the high contact pressures in the secondary shear zone. The second reason is that the Leidenfrost effect does not allow the infiltration of the fluid between the asperities because

of the evaporation mechanism before the contact with the surface [7].

Another work was carried out by Courbon et al. [8] consists of sphere-cylinder friction tests on a machining lathe. The authors concluded that the friction coefficient was indifferent for dry contact, under liquid nitrogen and nitrogen gas for Ti-6Al-4V and WC/Co friction without TiN coating. In the work of Pusavec et al. [9], friction tests state that the projection of LCO_2 alone tends to increase the friction coefficient. However, the coupling of LCO_2+oil and LCO_2+MoS_2 decreases the friction coefficient by 80% and even allows negative contact temperatures.

In the work of Yong and Ding [10], the effect of cryogenic quenching is studied on tungsten carbide with 8%wt Cobalt content. The results showed that the hardness and compressive strength are higher for the cryogenically quenched samples. The compressive residual stresses are greater and goes deeper beneath the surface. this is induced by the observed phase change of cobalt in WC/Co from α phase to a more compact ε phase.

The wear mechanisms encountered in extreme contact conditions of titanium alloys and nickel superalloys are abrasion, adhesion, and diffusion [11]. In this context, Tayeb et al. [12] have performed an experimental modeling by the method of response surfaces of the wear volume of Ti-5Al-4V-0.6Mo-0.4Fe (Ti-54) pins. The varied contact conditions were normal force, sliding velocity and test time. The tests concluded that cryogenic assistance decreases the wear volume and attenuates the effects of sliding speed, normal force and friction time. The dominant wear mechanisms are abrasion and delamination. Plate-like debris as well as brittle cracks are observed on the worn surface of Ti-54 pins [12].

There are three techniques for implementing cryogenic assistance in machining: extern projection, cryogenic quenching, and internal lubrication of cutting tools [13]. The modern development of new tools with internal channels for cryogenic media routing granted the possibility to spray cryogenic fluid to the closest from the chip formation zone or flank face. The spraying nozzles are included in the tool's functional faces (cutting face and flank face).

Several comparative studies have been conducted to optimize the benefits of cryogenic assistance [14]. Most of the results research converge on the external spray mode or the internal delivery of cryogenic fluid to optimise the liquid phase ration of the cryogenic media in contact with the tool-chip-workpiece system. In without identifying the effect of liquid nitrogen under extreme contact conditions. To identify the benefits of a liquid phase of cryogenic lubricant in the cutting zone, the entire tribological system is soaked in a cryogenic liquid bath.

To analyse the tribological aspects of cryogenic machining, an experimental simulation of the contact conditions has been carried out. Several friction tests were conducted to identify the effect of the cryogenic environment on the behavior of the tool-chip interface during machining. Pin-on-disk friction tests are carried out with different normal pressure and sliding speed conditions. The test bench is equipped with a vacuum cryogenic installation. The cryogenic fluid used is the liquid nitrogen LN_2 for its very low change of state temperature of -193°C and its abundance and ease of synthesis. The identification of the tribological and wear behavior is carried out in a LN_2 cryogenic bath in order to eliminate the projection effect.

2. Experimental setup

2.1. Conditions of tests

The performed friction tests consist of a pin-on-disk contact. The WC/Co pin translates vertically applying a normal pressure on the TA6V alloy disk which is driven in continuous rotation. The simulated normal pressures are derived from numerical modeling using the finite element method under Adaptive Lagrangian Eulerian (ALE) formulation. The material flow for a given cutting speed and feed rate applies a normal pressure field on the cutting face of the tool. At the tip, the pressures are of the order of 2.5 GPa and the velocities are very low and highly dependent of cutting parameter computed. Unlike the chip-tool separation zone at the end of contact where speeds are high with a low normal pressure.

The applied pressures and sliding speeds are equivalent to the friction conditions between the cutting tool and the chip during a real machining operation simulated by the numerical approach. To identify the tribological behavior under dry and cryogenic environments, 4 levels of pressure and sliding speed are selected in the test plan, see table 1.

Table 1. Design of friction tests

Linear sliding speed (m.min^{-1})	Pressure (MPa)	Normal force (N)
30	1000	5
60	1500	15
90	2000	35
120	2500	70

2.2. Investigated materials

The material of the disk is the alloy: Ti6Al4V-ELI Grade 5. A ribbon saw was used to cut the disks with a diameter of 70 mm and a thickness of 10 mm. To eliminate the effect of roughness on the tribological behavior, polishing operations with an abrasive disk were previously performed. The surface roughness of each disc does not exceed 0.3 µm. The 6 mm diameter friction balls are made of tungsten carbide WC/Co of grade 10 with 7% of cobalt. The pin's surface roughness is about 0.2 µm, see Fig.1.

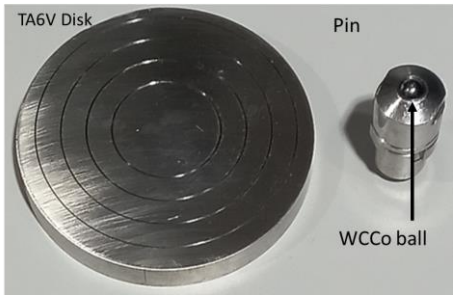

Fig. 1. Illustration of the two test specimens for the pin-on-disk tests.

2.3. Experimental procedure

The tribometer used is "BRUKER® UMT tribolab" with a DFG 10G load cell and a test range of 0 to 113 N, see Fig. 2a. A rotary lubrication module from the same manufacturer was installed for the cryogenic bath tests. The test bench can apply up to 2000 N of normal force and 5000 rpm in rotation speed.

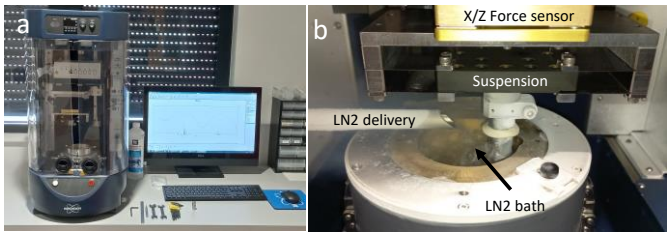

Fig. 2. (a) Brucker UMT tribometer; (b) Illustration of cryogenic bath tests with lubricant test module.

In order to guarantee a liquid level covering the friction zone, see Fig. 2b, a cryogenic installation was set up with storage and vacuum conveying, see Fig. 3. The nitrogen liquid is stored in a self-pressurized dewar at 0.5 bar. The cryogenic fluid circulates in a vacuum hose to ensure that the liquid phase reaches the cryogenic bath. The pressure regulation system allows to keep a pressure of 0.5 bar at the tank outlet during use. In this study, we aim to verify the effects of cryogenic liquid phase in the tool-chip interface. To achieve this condition, friction zone is soaked in a cryogenic bath to ensure the presence of liquid nitrogen between the surface before contact is established.

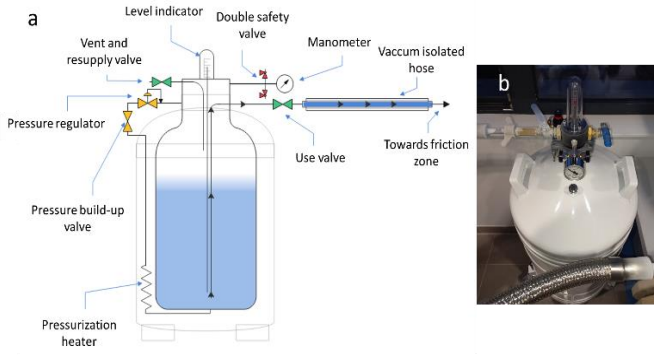

Fig. 3. (a) Schematic of the cryogenic installation of the test bench, (b) Illustration of the cryogenic installation.

The carriage driving vertically the pin is force regulated to ensure a stable normal contact pressure during the whole test. A friction length of 50 m is set for all friction tests. The digital force signal emitted by the test bench is then processed by a low-pass filter to minimize the noise measurement. A postprocessing script is executed to extract the average friction coefficient in a stable contact phase based on the fluctuation of the normal and friction force filtered signals. The experimental test plan executed in this study aim to identify the primary effect cryogenic liquid on the friction behavior. Every set of contact condition is tested once. The friction coefficient is computed according to the formula:

$$\mu = \frac{F_x}{F_z} \quad (1)$$

After friction tests, a wear volume characterization was performed. The friction tracks are scanned by interferometry at three equidistant points of measurement. The BRUKER® NP-FLEX interferometer with a super long working distance lens was used for the scan. The digital surfaces are processed via the Gwyddion software and then exported in (.asci) format to a python program for the calculation of the wear volume of the whole track. The size of the digital surfaces is large enough to encompass any heterogeneous morphology of the track. Other images from digital microscope and scanning electron microscope are made for the analysis of the results.

3. Results and discussion

3.1. Tribological behavior

Under dry contact configuration, high sliding speeds induce a decrease in the friction coefficient of 10 to 15% from 30 to 120 m.min^{-1}. See Fig. 4a. A decrease of 5 to 15% of the friction coefficient is noticed between the pressure of 1 GPa and 2.5 GPa, see Fig. 4b.

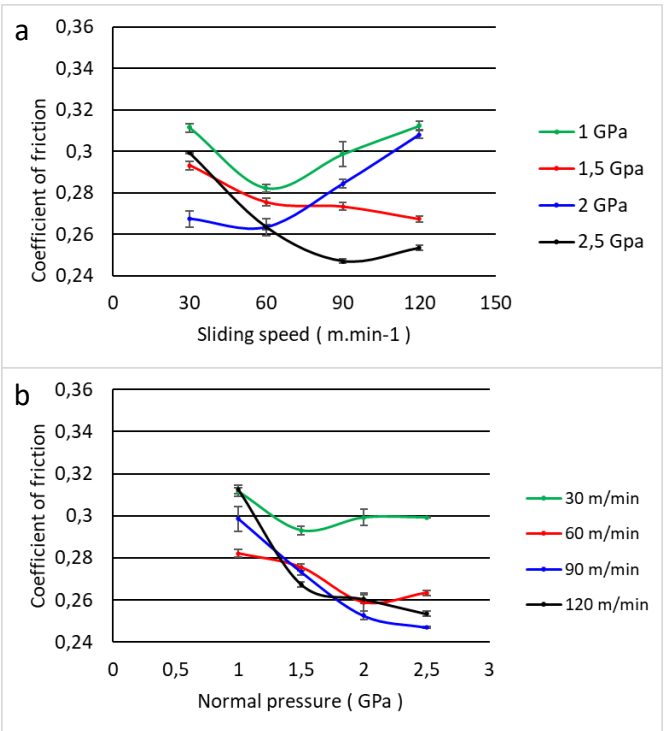

Fig. 4. Evolution of the friction coefficient under dry contact with: (a)- Sliding speed, (b) Pressure.

Several studies in the literature state that the high sliding speed systematically induces higher contact temperatures [9]. Moreover, the high contact pressure conditions lead to high temperature induced by severe plastic deformation of titanium alloy. This phenomenon is well known as the Taylor–Quinney effect which specifies plasticity-induced heating or fraction of plastic work converted to heat. A thermal softening effect can then be induced by the generated heat in the contact zone favors the plastic flow of the Ti-6Al-4V alloy to the lateral edges. At the same time the plastic deformation generates the strain hardening of the track valley and then reduces the penetration of the tungsten carbide asperities in the disk's material. In consequence, a reduction of the contact reaction force occurs, inducing friction coefficient drop. A saturation of the friction coefficient at 0.25 is observed beyond 60 m.min^{-1} of sliding speed effect and 1.5 GPa for normal pressure effect.

The measurement deviation obtained in dry friction tests doesn't exceed 2% of the minimum average friction coefficient recorded. According to the literature [1], standard deviation in friction coefficient is relevant to sliding distances. All signals recorded reach their maximum between 0 to 3 m of friction distance. Beyond that point, a brief stabilization phase take place till the test's end at 50 m sliding distance. The post process of the friction signal is focused on the stable phase of the friction force and normal force signals recorded. The highest deviation in dry contact test is obtained at lowest sliding speed and high normal pressure, that observation is related to the ploughing effect observed when contact is made under high normal pressure and low sliding.

Under cryogenic environment, the friction coefficient increases with the sliding speed except for the speed of 30 m.min^{-1}. Between 60 and 120 m.min^{-1}, the friction coefficient increases by 15% on average for the three normal pressures 1, 2, and 2.5 GPa, see Fig. 5.

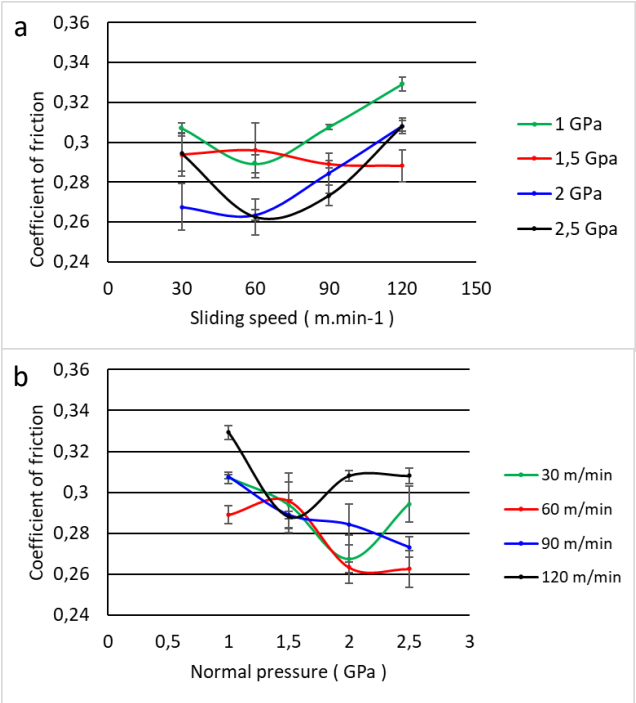

Fig. 5. Evolution of the friction coefficient in cryogenic bath friction with: (a) Sliding speed, (b) Pressure.

Friction test in cryogenic environment showed a higher deviation in average friction coefficient extraction compared to dry contact. The deviation of cryogenic friction coefficient under sliding speeds 30, 60 and 90 m.min^{-1} reach 0.011 which represent 5% of the lowest mean friction coefficient obtained. While sliding at 120 m.min^{-1}, the deviation doesn't exceed 2%, similarly to the dry contact case.

The thermal softening effect observed in dry friction is eliminated by the low temperatures in the cryogenic bath. The effect of cryogenic temperatures on the microstructure induces embrittlement of the Ti-6Al-4V asperities which subsequently undergo brittle fracture. The higher the sliding speed, the higher the microscopic shocks between asperities. The tangential force component and the friction coefficient are therefore increasing with high sliding speeds.

3.2. Wear volume and surface integrity

In dry contact, the wear volume increases with normal pressure. Quantitatively, the wear volume increases by 50% when increasing the pressure from 1 GPa to 2.5 GPa under dry condition, see Fig. 6. However, the sliding speed has no effect on the wear volume. The deviation of the track worn volume observed in dry contact results is mainly relevant to instable contact regime caused by ploughing and chattering effects.

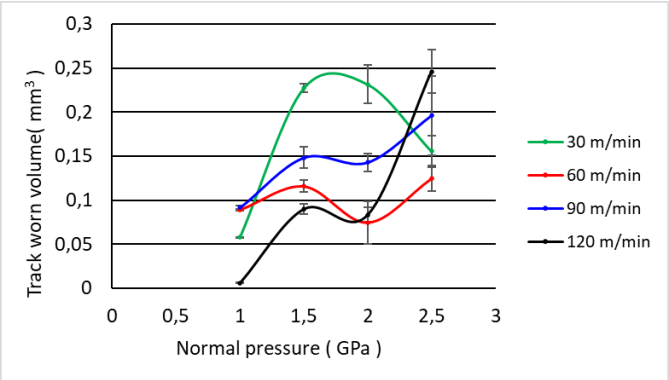

Fig. 6 Effect of normal pressure on wear volume in dry contact condition.

A chattering effect is observed on the friction track topographies with 30 m.min^{-1} sliding speed. The contact is not continuous. It has been noticed that low speeds coupled with high pressures in dry contact induce the chattering of the disk surface by the pin. The contact surface is not stable during the friction and thus leaves a characteristic trace, see Fig. 7. Other studies have found similar surface morphologies in dry contact [15].

The wear volume in cryogenic bath is mainly affected by the normal pressure. In contrast to dry friction, all test conditions induced a lower wear volume in cryogenic bath friction. The wear is harshly reduced, but the effect of pressure is very noticeable. The application of high pressures induces a wear volume of up to 90% for the test at 120 m.min^{-1}, see Fig. 8. The sliding speed has no effect on the wear volume.

The deviation of the track worn volume observed in cryogenic contact doesn't exceed 3%. That drop in deviation is

relevant to friction track homogenous wear. That observation prove that less non-steady phenomenon like damping is noticed while cryogenic environment is established. The surface topography conducted are confirming that statement.

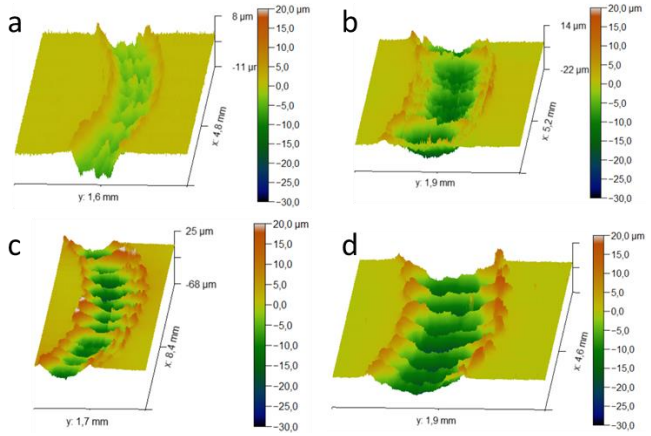

Fig. 7 Surface topography scanned by interferometry for dry contact with condition: (a)- V = 30 m.min^{-1}, P = 1 GPa; (b)- V = 120 m.min^{-1}, P = 1 GPa; (c)- V = 30 m.min^{-1} , P = 2.5 GPa ; (d)- V = 120 m.min^{-1} , P = 2.5 GPa.

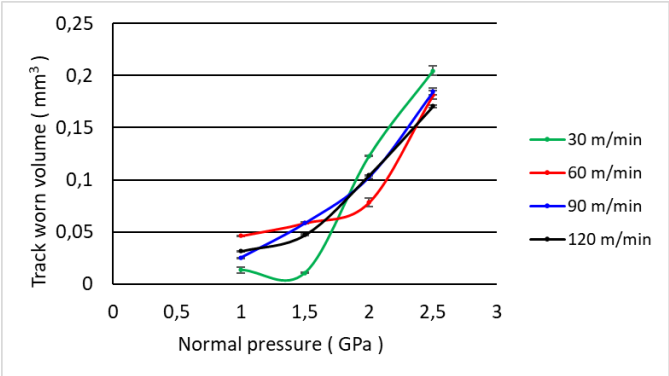

Fig. 8 Effect of normal pressure on wear volume in cryogenic bath friction.

Observing the cryogenic friction track topographies, the tracks hollow depths are significantly lower in cryogenic friction. However, for the lowest normal pressure of 1 GPa, the disk tracks are like those of dry friction. The chatter is reduced but still concerns the same high pressure and low sliding speed conditions. The lateral ridges are absent from the wake for the pressure 2.5 GPa and 120 m.min^{-1}, see Fig. 9.

The effect of cryogenic temperatures on the micro-hardness of Ti-6Al-4V justify the low depths of tracks in cryogenic bath. The literature states that exposure of the two-phase (α+β) titanium alloys such as Ti-6Al-4V to cryogenic temperatures causes a layer of β-Ti phase concentration below the 40 µm surface. The β-Ti phase is characterized by a centered cubic type of crystal lattice providing a gain in micro-hardness.

The absence of beads indicates that the material has weakened in the cryogenic bath. The plasticization of the material is minimal du to reduced thermal softening in cryogenic temperatures. The effect of cryogenic temperatures on the thermomechanical behavior of the TA6V alloy favors indirectly abrasive wear that reduces adhesion. The low level of the topography is reached gradually turn after turn. On the other hand, in dry friction, the initial indentation of the pin applying the normal force induces a material plastic flow from the beginning of the friction. With less sliding speed, the thermal softening is lower, and the contact tends to chatter.

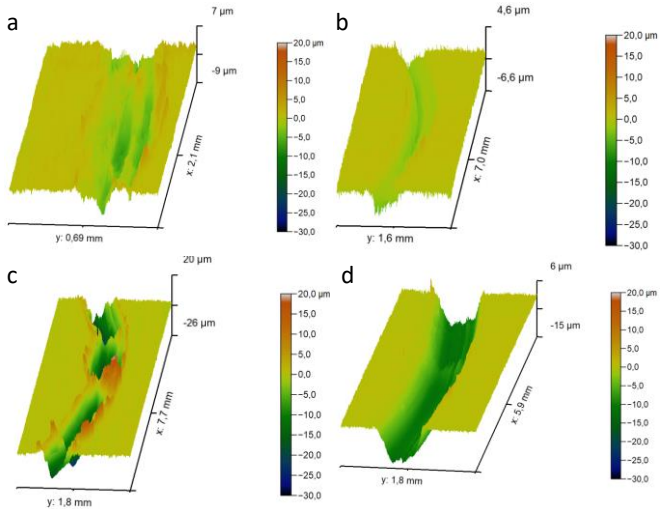

Fig. 9 Surface topography scanned by interferometry for cryogenic contact with condition: (a)- V = 30 m.min^{-1}, P = 1 GPa; (b)- V = 120 m.min^{-1}, P = 1 GPa; (c)- V = 30 m.min^{-1} , P = 2.5 GPa ; (d)- V = 120 m.min^{-1} , P = 2.5 GPa.

The surface topography obtained for cryogenic friction under pressure 2.5 GPa and with 120 m.min^{-1} in sliding speed is very smooth and does not reflect any sign of material tearing due to adhesion to the pin. The image under the optical scanning microscope consolidates the veracity of the phenomenon of embrittlement of the contact asperities under cryogenic environment, see Fig. 10. The SEM images revealed more debris in the hollow of the sliding track tested in cryogenic environment. The plastic tangential material flow is clearly reduced in cryogenic friction test. In addition to that, we can easily identify some surface cracks in the image of the cryogenic bath friction track.

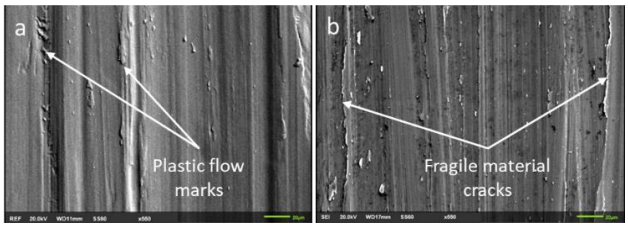

Fig. 10. SEM images of the sliding track's hollows in (a) Dry contact;(b) Cryogenic bath contact.

The wear mechanisms observed on the surface of the WC/Co ball are adhesion and abrasion. Cryogenic friction induces a low adhesion on the pin and decreases the diameter of the wear mark. The low temperatures reached in cryogenic friction thermally limit adhesion and abrasion. However, the gain in hardness of tungsten carbide under cryogenic temperature considerably attenuates abrasion in comparison with the pin used for dry contact tests, see Fig. 11. The diameter of the worn area of the pin's surface had increased by 150%

when applying 2.5 GPa compared to 1 GPa of normal pressure. Cryogenic bath condition induces 85% smaller worn surface compared to dry contact tests indifferently from the normal pressure applied.

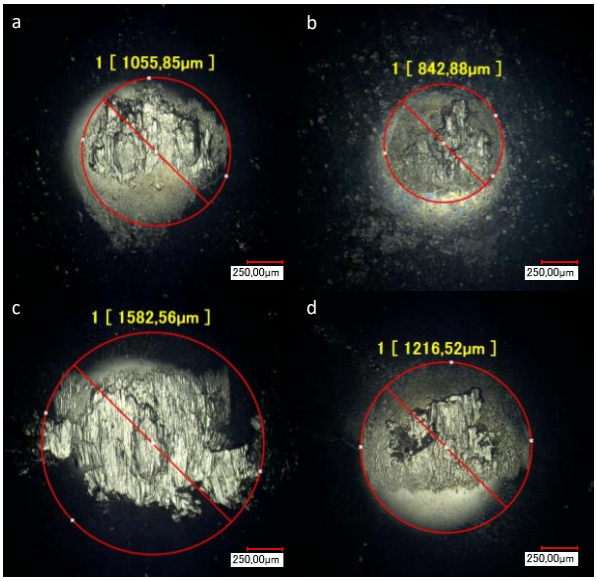

Fig. 11. Microscope observation of the pin surface after friction test with condition V =30 m.min^{-1}, P = 2500 GPa in (a) Dry contact;(b) Cryogenic bath contact; and with V = 120 m/min^{-1}, P = 2500 GPa in (c) Dry contact ; (d) Cryogenic bath contact

4. Conclusion

The experimental work consisted of pin-on-disk friction tests in dry and cryogenic conditions. Sliding speed and normal pressure were chosen to fit the extreme load in cryogenic assisted machining. Work materials were the TA6V alloy for the disks and WC/Co for the pins. Friction coefficient, wear volume and surface morphology were investigated to highlight the cryogenic effect on extreme machining contact mechanisms. Several cryogenic effect on the tribological and wear behaviors were notified:

- The LN_2 bath friction leads to low contact temperature and limits the thermal softening effect. This phenomenon is replaced by rigid fragile asperities contact during tests with cryogenic bath. The friction coefficient increases with the highest sliding speed in LN_2 bath instead of decreasing as observed in dry contact.
- Increasing normal pressure induces severe plastic deformation outside the friction track. The strain hardening of the confined titanium alloy under the pin leads to a decrease in the friction coefficient level with high contact pressure.
- The contact under high pressures induces a higher wear volume in cryogenic friction. The gain in hardness of the tungsten carbide WC/Co and the embrittlement of the titanium alloy Ti-6Al-4V exposed to low temperatures tends to gradually erode the surface without plasticizing the titanium alloy.
- The friction in cryogenic bath drastically decreases the adhesion and the abrasion surface size of the worn pin.

Acknowledgements

The authors would like to thank the ‘Région Grand-Est’ and BPI France for their funding of the FCCN-IP AAP-PSPC project which constitutes the framework of the work carried out.

References

[1] M. Bogdan-Chudy et al., « Tribological and thermal behavior with wear identification in contact interaction of the Ti6Al4V-sintered carbide with AlTiN coatings pair », Tribol. Int., vol. 167, p. 107394, mars 2022, doi: 10.1016/j.triboint.2021.107394.

[2] A. Taghizadeh Tabrizi, H. Aghajani, et F. Farhang Laleh, « Tribological characterization of hybrid chromium nitride thin layer synthesized on titanium », Surf. Coat. Technol., vol. 419, p. 127317, août 2021.

[3] D. Zindani and K. Kumar, “A brief review on cryogenics in machining process,” SN Applied Sciences, vol. 2, no. 6, 2020.

[4] S. Y. Hong, I. Markus, and W. cheol Jeong, “New cooling approach and tool life improvement in cryogenic machining of titanium alloy Ti-6Al-4V,” International Journal of Machine Tools and Manufacture, vol. 41, no. 15, pp. 2245–2260, 2001, doi: 10.1016/S0890-6955(01)00041-4.

[5] C. GIANESE, “Propriétés des fluides cryogéniques,” Ref : TIP204WEB - “Froid industriel.” 2015.

[6] S. Hong, “Lubrication mechanisms of LN2 in ecological cryogenic machining,” Machining Science and Technology, vol. 10, no. 1, pp. 133–155, 2006, doi: 10.1080/10910340500534324.

[7] B. S. Gottfried, C. J. Lee, and K. J. Bell, “The leidenfrost phenomenon: film boiling of liquid droplets on a flat plate,” International Journal of Heat and Mass Transfer, vol. 9, no. 11, pp. 1167–1188, 1966.

[8] C. Courbon, F. Pusavec, F. Dumont, J. Rech, and J. Kopac, “Tribological behaviour of Ti6Al4V and Inconel718 under dry and cryogenic conditions - Application to the context of machining with carbide tools,” Tribology International, vol. 66, pp. 72–82, 2013, doi: 10.1016/j.triboint.2013.04.010.

[9] F. Pušavec, L. Sterle, M. Kalin, D. Mallipeddi, and P. Krajnik, “Tribology of solid-lubricated liquid carbon dioxide assisted machining,” CIRP Annals, vol. 69, no. 1, pp. 69–72, 2020, doi: 10.1016/j.cirp.2020.04.033.

[10] J. Yong and C. Ding, “Effect of cryogenic treatment on WC-Co cemented carbides,” Materials Science and Engineering A, vol. 528, no. 3, pp. 1735–1739, 2011, doi: 10.1016/j.msea.2010.11.009.

[11] J. Caudill, J. Schoop, and I. S. Jawahir, “Producing sustainable nanostructures in Ti-6Al-4V alloys for improved surface integrity and increased functional life in aerospace applications by cryogenic burnishing,” Procedia CIRP, vol. 80, pp. 120–125, 2019, doi: 10.1016/j.procir.2018.12.022.

[12] N. S. M. El-Tayeb, T. C. Yap, and P. V. Brevern, “Wear characteristics of titanium alloy Ti54 for cryogenic sliding applications,” Tribology International, vol. 43, no. 12, pp. 2345–2354, 2010, doi: 10.1016/j.triboint.2010.08.012.

[13] G. Germain, A. Morel, and A. Morel, “Assistance cryogénique en usinage,” Techniques de l’ingénieur, vol. 1, no. 0, 2016.

[14] I. S. Jawahir et al., “Cryogenic manufacturing processes,” CIRP Annals - Manufacturing Technology, vol. 65, no. 2, pp. 713–736, 2016, doi: 10.1016/j.cirp.2016.06.007.

[15] H. ben Abdelali, “Caractérisation et modélisation des mécanismes tribologiques aux interfaces outils-pièces-copeaux en usinage à sec de l’acier C45,” 2013. [Online]. Available: https://tel.archives-ouvertes.fr/tel-00805316